Quantum efficiency coefficient for photogeneration of carriers in gallium sulphide single crystals

2007 J. Phys.: Condens. Matter 19 196210

(http://iopscience.iop.org/0953-8984/19/19/196210)

IOP PUBLISHING JOURNAL OF PHYSICS: CONDENSED MATTER

J. Phys.: Condens. Matter **19** (2007) 196210 (14pp) doi:10.1088/0953-8984/19/19/196210

Quantum efficiency coefficient for photogeneration of carriers in gallium sulphide single crystals

M Szałajko[1] **and M Nowak**

Department of Solid State Physics, Silesian Technical University, PO BOX 221, PL 40019 Katowice, Poland

E-mail: maria.szalajko@polsl.pl

Received 13 December 2006, in final form 14 December 2006
Published 19 April 2007
Online at stacks.iop.org/JPhysCM/19/196210

Abstract

This paper presents investigations of the quantum efficiency coefficient for the photogeneration of carriers in gallium sulphide (GaS) single crystals. Therefore the spectral dependences (between 420 and 550 nm) of photoconductivity (σ_{PC}) were measured for temperatures from 80 to 333 K and for different light intensities. Since σ_{PC} depends on the absorption and reflection coefficients, these parameters were determined in the same range of temperatures. The least-squares method was applied to fit the experimental σ_{PC} data with appropriate theoretical dependence. From this fitting, spectral dependences of quantum efficiency coefficients for different temperatures and different light intensities were obtained. A comparison of the values of absorption coefficient obtained from the measurements of optical transmittance and from evaluation of the quantum efficiency coefficient is presented.

1. Introduction

Gallium sulphide (GaS) is one of the less studied compounds of the III–VI family. It is a typical layered semiconductor and it is a promising material for optoelectronics devices, e.g. GaS may be used in near-blue-light emitters [1] since it has a wide band gap (E_g (295 K) $= 2.5$ eV and E_g (80 K) $= 2.62$ eV [2]). GaS crystallizes in the so-called β-polytype that carries the symmetry properties of the D^4_{6h} space group [3]. The optical axis c is perpendicular to the layers. The intralayer interactions are of covalent type with small ionic contribution [4]. The layers are connected with van der Waals forces [4].

One of the features of merit of semiconductors and heterocontacts of semiconductors with organic substances in optoelectronics is the quantum efficiency coefficient β for photogeneration of excess carriers [5–8]. This coefficient describes the number of free carriers generated by one photon. It is especially needed in the description of, for

[1] Author to whom any correspondence should be addressed.

example, the photoconductivity (σ_{PC}) of the semiconductor. Some results of investigations of photoconductivity in GaS single crystals at room temperature were presented in [9]. The authors of [9] show that σ_{PC} is not a linear function of light intensity, and it is described by a power-law equation. Unfortunately they gave no information about the photon energy of the incident light and they did not take into consideration the β coefficients. In fact, no literature is available on β concerning the properties of GaS. So, it seems to be useful to evaluate the spectral dependences of the coefficients γ of the power-law dependence of σ_{PC} on the light intensity for different temperatures and to calculate the quantum efficiency coefficients for photogeneration of carriers in GaS. To analyse the photoelectric properties of a semiconductor one needs information on its optical properties. Therefore in this paper the optical and photoconductivity investigations have been performed on the same material.

2. Experimental set-up

All the measurements were carried out on n-type GaS single crystals grown by the Bridgman–Stockbarger method at the University of Bari, Italy. The details of the crystal growth have been reported elsewhere [10, 11]. The present measurements were performed on the samples obtained by cleaving the monocrystals along the plane perpendicular to the c-axis. The platelets had about 0.5×0.5 cm^2 area and were 90 μm thick. Due to this thickness the interference effect of radiation internally reflected in the samples was avoided in the spectral range investigated. The electrical contacts for photoconductivity measurements had been made in the planar configuration with silver paste. They were checked to be ohmic at low voltages and to show a symmetrical behaviour with respect to the voltage polarity. For the temperature measurements an R2205 cryogenic microminiature refrigeration II-B system (MMR Technologies) based on the Joule–Thomson effect was used. Temperatures were controlled with 0.1 K uncertainty using a K7701 (MMR Technologies) temperature controller. The photoconductivity was measured using a Keithley 617 electrometer. The investigations were performed as a function of wavelength from 420 ($h\nu = 2.95$ eV) to 550 nm ($h\nu = 2.25$ eV) using an SPM2 monochromator (Carl Zeiss) with 750 W halogen lamp. Some of the measurements were done using a Reliant 50S argon laser (Laser Physics) with photon energy $h\nu = 2.54$ eV ($\lambda = 488$ nm). Neutral filters UV–NIR-FILTER-250–2000 nm (Quartzglas-Substrate, Oriel) were used to change the light intensity. The last quantity was measured using an S-2387 silicon photodiode (Hamamatsu) and a PM 150 laser beam detector with a Powermax 5200 meter (Molectron-Coherent). The illumination was perpendicular to the layers of investigated samples and was changed from 10^{17} to 10^{22} photons m^{-2} s^{-1}. Acquisition of the data and control of the wavelength of radiation were realized using a PC computer with IEEE 488 bus.

The optical transmittance (T_0) and reflection (R_0) were measured using a PC2000 spectrophotometer (Ocean Optics Inc.) with master and slave cards with 600 lines grating (blazed at 500 and 400 nm respectively). The spectrophotometer was equipped with appropriate waveguide cables and reflection Y probe as well as with a deuterium–halogen light source (DH2000-FHS, from Sentronic GmbH). The sample was mounted in the optical D2209 chamber of the R2205 cryogenic microminiature refrigeration II-B system. The multiple averaged spectral characteristics containing 2048 data points for different wavelengths (in the range 200–850 nm) were registered at various temperatures using a PC and the OOI-Base program from Ocean Optics Inc.

The investigations of photoconductivity as well as of the optical reflection and transmittance were carried out for the same samples and in the same temperature range from 80 to 333 K.

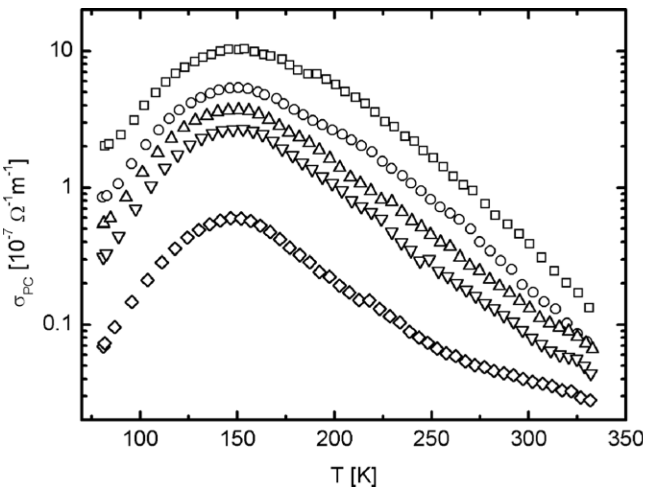

Figure 1. Photoconductivity of GaS as a function of temperature for photon energy $h\nu = 2.54$ eV and for different intensities of illumination ((□) $I_0 = 3.45 \times 10^{21}$ photons m^{-2} s^{-1}, (○) $I_0 = 1.4 \times 10^{21}$ photons m^{-2} s^{-1}, (△) $I_0 = 8 \times 10^{20}$ photons m^{-2} s^{-1}, (▽) $I_0 = 5.1 \times 10^{20}$ photons m^{-2} s^{-1}, (◇) $I_0 = 9.25 \times 10^{19}$ photons m^{-2} s^{-1}).

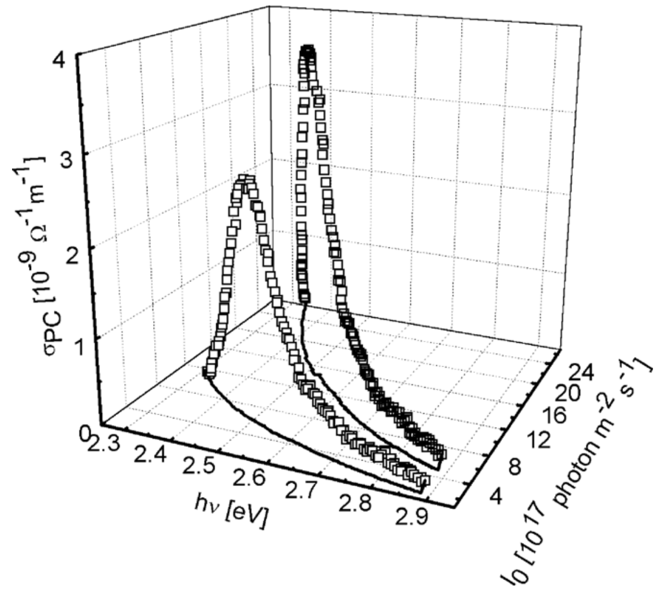

Figure 2. Experimental data of spectral dependences of photoconductivity of GaS at 333 K. Solid curves show the spectral dependences of illumination intensities.

3. Experimental results

The temperature dependences of σ_{PC} in the GaS sample illuminated by an argon laser ($h\nu = 2.54$ eV) for different light intensities are shown in figure 1. The σ_{PC} response attains a maximum at a temperature about 150 K.

The results of σ_{PC} investigations for the sample illuminated by the monochromator at $T = 333$ K are presented in figure 2. Such illumination strongly depends on the wavelength. In figure 2 the solid curves represent the spectral dependences of the intensity of light incident upon the sample from the monochromator used. To normalize σ_{PC} data for constant illumination, the experimental results were least-squares fitted with the semiempirical power equation [6]:

$$\sigma_{PC}(h\nu, T) = A(h\nu, T) I_0^{\gamma(h\nu,T)} \quad (1)$$

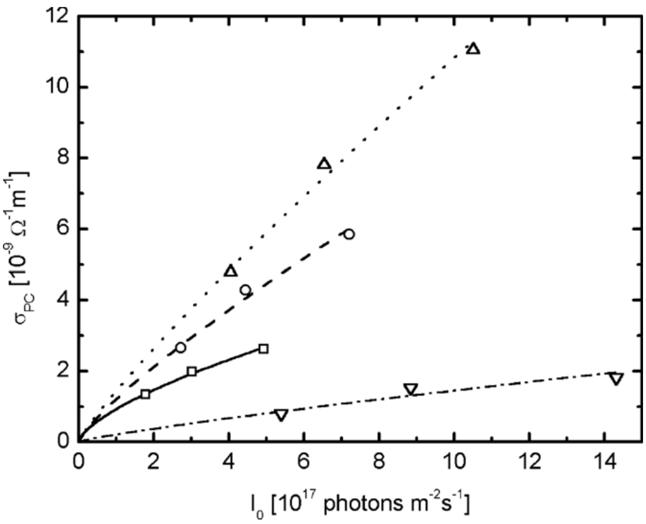

Figure 3. Photoconductivity of GaS as a function of light intensity at $T = 80$ K for different photon energies ((□) $h\nu = 2.88$ eV, (○) $h\nu = 2.75$ eV, (Δ) $h\nu = 2.64$ eV, (∇) $h\nu = 2.54$ eV); solid and dashed curves represent least-squares fitted semiempirical dependence (1); the values of fitted power coefficients $\gamma(h\nu, T)$ are presented in figure 5.

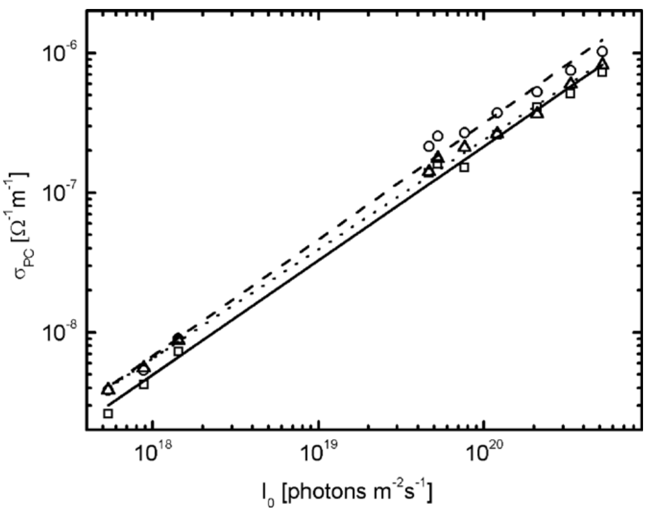

Figure 4. Photoconductivity of GaS as a function of light intensity for photon energy $h\nu = 2.54$ eV for different temperatures ((□) $T = 120$ K, (○) $T = 150$ K, (Δ) $T = 173$ K); solid and dashed curves represent least-squares fitted semiempirical dependence (1); the values of fitted power coefficients $\gamma(h\nu, T)$ are presented in figures 5 and 6.

where I_0 is the incident light intensity, and $\gamma(h\nu, T)$, $A(h\nu, T)$ are coefficients which depend on photon energy and temperature.

Figures 3 and 4 present the σ_{PC} data as a nonlinear function of light intensity for different photon energies and different temperatures, respectively. The solid and dashed curves represent the semiempirical dependence (1) least-squares fitted to the experimental data. The fitting is rather good. The values of power coefficients $\gamma(h\nu, T)$ evaluated using this fitting are shown in figures 5 and 6.

The spectral and temperature characteristics of the power coefficient $\gamma(h\nu, T)$ are presented in figures 5 and 6. The values of γ change with photon energies and temperatures from about 0.2 to 1. The spectral characteristics for lower temperatures begin at higher photon energies due to the changes of energy gap of the investigated GaS. The lowest values of γ are observed for the highest temperature, 333 K (figures 5 and 6). One can see that the linear proportionality between photoconductivity and the intensity of illumination as well as the independence of recombination velocity of excess carriers on their concentration is observed

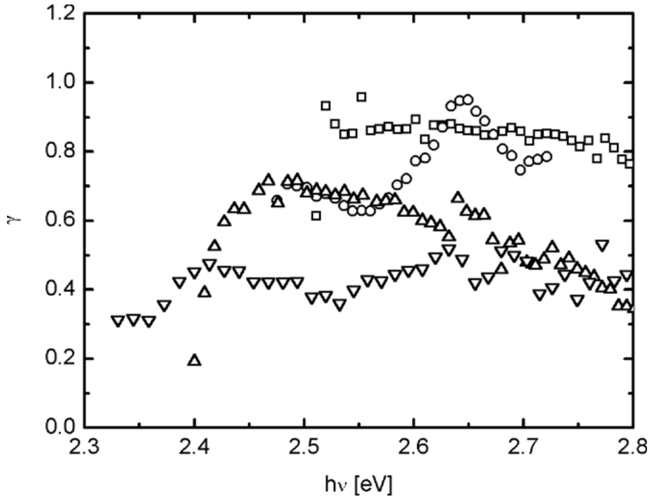

Figure 5. Spectral dependences of power coefficient $\gamma(h\nu, T)$ from equation (1) least-squares fitted to the experimental data of photoconductivity of GaS for different temperatures ((□) $T = 80$ K, (○) $T = 238$ K, (△) $T = 293$ K (▽)$T = 333$ K).

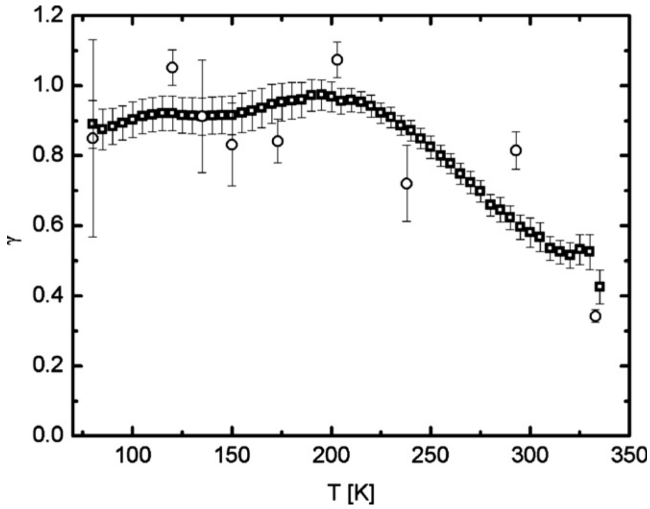

Figure 6. Power coefficient $\gamma(h\nu, T)$ from equation (1) least-squares fitted to the experimental data of photoconductivity of GaS as a function of temperature for photon energy $h\nu = 2.54$ eV. (□) Values obtained for laser illumination, (○) values obtained for monochromator.

at lower temperatures (e.g. below 200 K for $h\nu = 2.54$ eV; figure 6) and for energies only a little smaller than the energy gap of GaS (figure 5). Above 200 K the values of γ decrease, and they attain a value of about 0.5 at 333 K. These values are well comparable with the values of $\gamma(h\nu = 2.54 \text{ eV}, T)$ obtained in experiments with the monochromator (figure 6). The differences observed in figure 6 may be understood by taking into account the fact of much smaller light intensities and greater uncertainties in the second experiment.

Using the determined values of $A(h\nu, T)$ and $\gamma(h\nu, T)$, the spectral characteristics of $\sigma_{PC}(h\nu, T)$ were normalized for various constant light intensities. In figure 7 the typical, normalized $\sigma_{PC}(h\nu, I_0, T = 80 \text{ K})$ dependences are compared with the experimental data.

The spectral dependences of σ_{PC} of GaS normalized for constant light intensity ($I_0 = 6 \times 10^{17}$ photons m^{-2} s^{-1}) are presented in figure 8 for different temperatures. The shift of the spectral characteristics of σ_{PC} with the increase of temperature is connected with changes of the energy gap of the investigated material. Additionally, one can see that for each temperature a relatively low σ_{PC} signal also occurs for photon energies smaller than the energy gap. σ_{PC} attains a maximum value for photon energy higher than the band gap and decreases with

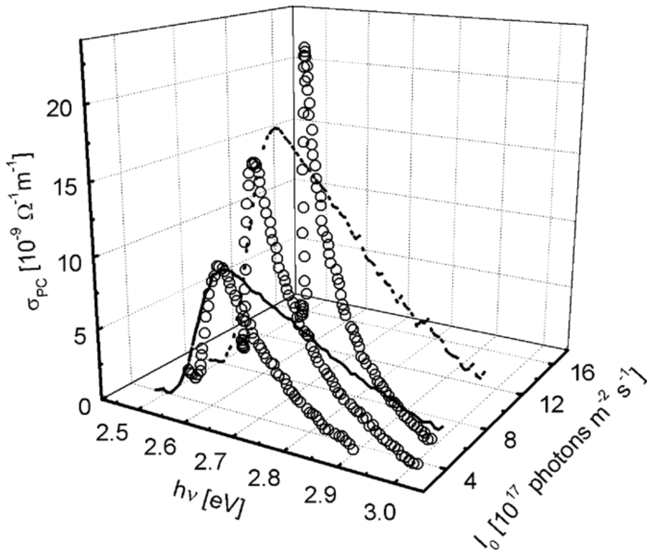

Figure 7. Experimental data (○) and normalized spectral characteristics of photoconductivity of GaS at $T = 80$ K for constant light intensities (solid and dot curves for $I_0 = 4 \times 10^{17}$ photons m^{-2} s^{-1} and $I_0 = 8 \times 10^{17}$ photons m^{-2} s^{-1}, respectively).

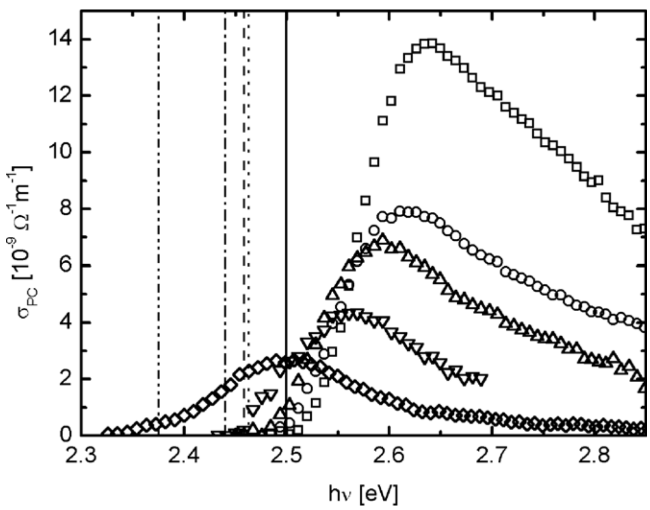

Figure 8. Influence of temperature on the normalized for $I_0 = 6 \times 10^{17}$ photons m^{-2} s^{-1} spectral characteristics of photoconductivity of GaS ((□) $T = 80$ K, (○) $T = 120$ K, (△) $T = 150$ K, (▽) $T = 203$ K, (◇) $T = 333$ K). Vertical lines indicate the indirect energy gaps determined from the spectral characteristics of absorption (see figure 15) for different temperatures ((——) $T = 80$ K, (- - - -) $T = 120$ K, (· · · · · ·) $T = 150$ K, (— · —) $T = 203$ K, (— · · —) $T = 333$ K).

increasing $h\nu$. There is a typical spectral dependence in the case of surface recombination of the excess carriers [12]. The decrease of temperature increases the maximum at spectral characteristics of σ_{PC} (figure 8). The temperature dependences of σ_{PC} for different photon energies are presented in figure 9. These dependences are complicated, due to the simultaneous influence of many variables on photoconductivity. Additionally, the same photon energy can

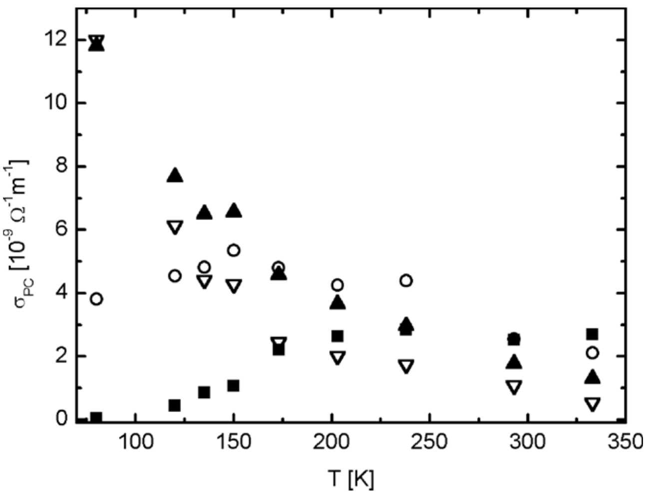

Figure 9. Influence of photon energy on temperature dependences of photoconductivity of GaS normalized for $I_0 = 6 \times 10^{17}$ photons m^{-2} s^{-1}; ((■) $h\nu = 2.5$ eV, (○) $h\nu = 2.54$ eV, (▲) $h\nu = 2.6$ eV, (▽) $h\nu = 2.7$ eV).

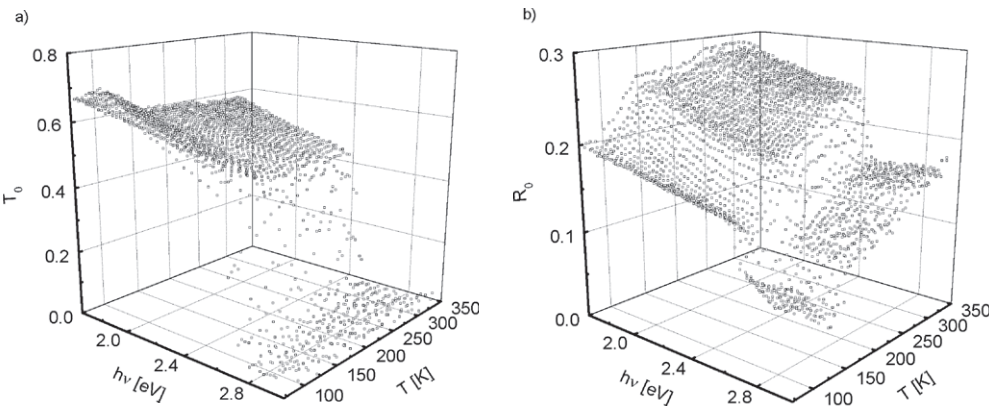

Figure 10. Spectral dependences of transmittance $T_0(h\nu, T)$ (a) and reflection $R_0(h\nu, T)$ (b) coefficients of GaS for different temperatures.

be smaller than the energy gap E_g at temperature T_1 and greater than E_g at higher temperature, T_2. It can be observed that for greater photon energies σ_{PC} only decreases with increasing temperature (see e.g. the results for $h\nu = 2.7$ eV in figures 8 and 9). For smaller photon energy (e.g. $h\nu = 2.54$ eV), σ_{PC} increases with increasing temperature, attains a maximum and then decreases (figures 1, 8 and 9).

Since the values of reflectivity $R_0(h\nu, T)$ and absorption coefficients $\alpha(h\nu, T)$ must be used to describe the σ_{PC} signal, the optical properties of GaS have also been investigated. The results of measurements of spectral dependences of optical transmittance $T_0(h\nu, T)$ and reflection $R_0(h\nu, T)$ are presented in 3D figure 10.

The obtained values of T_0 and R_0 were used to calculate the absorption coefficient $\alpha(h\nu, T)$ and the real part of the refractive index $n(h\nu, T)$, by applying the method presented in [13] for each photon energy and temperature of the sample. This method uses the appropriate formulae for transmittance and reflection of light in a thick sample without interference of internally reflected radiation. The determined spectral dependences of $n(h\nu, T)$ and $\alpha(h\nu, T)$ are presented in figure 11.

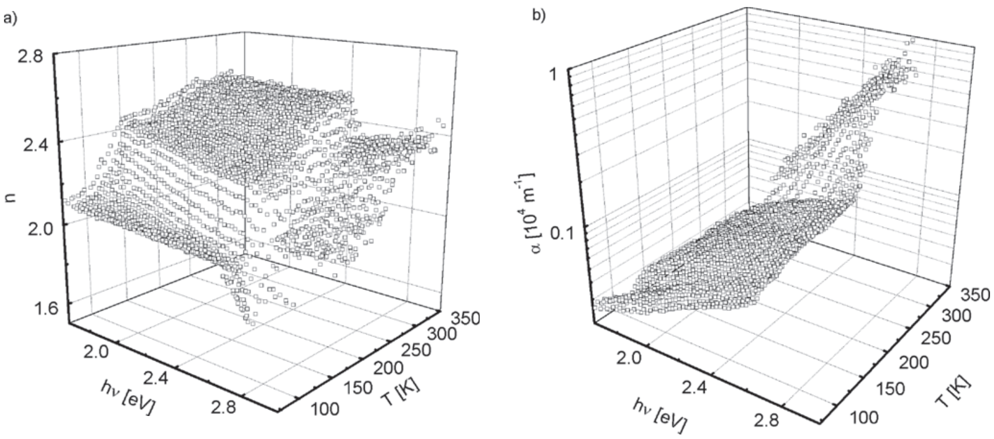

Figure 11. Spectral dependences of the real part of the refractive index $n(h\nu, T)$ (a) and absorption coefficient $\alpha(h\nu, T)$ (b) of GaS for different temperatures.

4. Discussion of the experimental results

The change of recombination velocity with the increase of excess carrier concentration evokes the cumbersome theoretical description of nonlinear dependence of σ_{PC} on the illumination intensity. However, in the first approximation of this problem, one can take into consideration different values of recombination parameters (i.e. diffusion length L, surface recombination velocities s_1 and s_2 at the front and back surfaces of the sample) for each intensity of illumination. In such a case, the photoconductivity can be described by the theory presented in for example [12].

$$\sigma_{\mathrm{PC}} = \frac{we\left(\mu_{\mathrm{n}}+\mu_{\mathrm{p}}\right) I_0\beta}{D}\frac{K}{W^2-K^2}\frac{1}{W} \times \left[\frac{(K-S_2)(W-S_1)\left(1-\mathrm{e}^{-W}\right)\mathrm{e}^{-K}+(K+S_1)(W+S_2)\left(1-\mathrm{e}^{W}\right)}{(W+S_1)(W+S_2)\,\mathrm{e}^{W}-(W-S_1)(W-S_2)\,\mathrm{e}^{-W}} - \frac{(K-S_2)(W+S_1)\left(1-\mathrm{e}^{-W}\right)\mathrm{e}^{-K}+(K+S_1)(W-S_2)\left(1-\mathrm{e}^{-W}\right)}{(W+S_1)(W+S_2)\,\mathrm{e}^{W}-(W-S_1)(W-S_2)\,\mathrm{e}^{-W}} + \frac{W}{K}\left(1-\mathrm{e}^{-K}\right)\right] \tag{2}$$

where $S_1 = s_1 w/D$, $S_2 = s_2 w/D$ are dimensionless surface recombination velocities on the front and back surfaces, $K = \alpha w$ is the dimensionless absorption coefficient, $W = w/L$ the dimensionless sample thickness, w the sample thickness, μ_n, μ_p the electron and hole mobilities, β the quantum efficiency coefficient for photogeneration of carriers, $D = D_{\mathrm{p}} b \frac{n_{0\mathrm{p}}+n_{0\mathrm{n}}}{n_{0\mathrm{p}}+bn_{0\mathrm{n}}}$ the ambipolar diffusion coefficient of carriers, D_p the diffusion coefficient of holes, and $b = \mu_n/\mu_p$, $n_{0\mathrm{p}}$, $n_{0\mathrm{n}}$ the equilibrium concentrations of electrons and holes.

This theory is based on the following assumptions: local charge neutrality in the sample; uniformly illuminated slab of semiconductor, infinite in the x and z directions; the bulk photogeneration rate is a function of y only; a steady state exists; the light intensity ensures small injection levels. Additionally it is assumed that surface recombination rates on both front and back surfaces of the sample are constant [12].

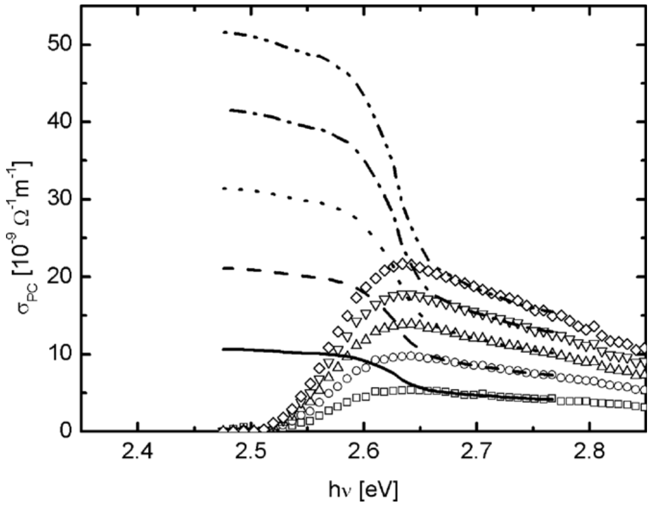

Figure 12. Normalized for different light intensities spectral characteristics of photoconductivity of GaS at 80 K ((□) $I_0 = 2 \times 10^{17}$ photons m^{-2} s^{-1}, (○) $I_0 = 4 \times 10^{17}$ photons m^{-2} s^{-1}, (△) $I_0 = 6 \times 10^{17}$ photons m^{-2} s^{-1}, (▽) $I_0 = 8 \times 10^{17}$ photons m^{-2} s^{-1}, (◇) $I_0 = 10^{18}$ photons m^{-2} s^{-1}). Solid and chained curves represent theoretical dependences (4) calculated for the values of the fitted parameters A_{PC} and S given in tables 1 and 2 and for the assumed $\beta = 1$.

The quantum efficiency coefficient for intrinsic photogeneration of carriers has the following definition (see e.g. [7]):

$$\beta = \frac{\alpha_\beta}{\alpha}\eta \tag{3}$$

where α represents the total absorption coefficient which affects the spatial distribution of radiation in a sample and is determined from the measurements of optical transmittance, α_β is the absorption coefficient describing absorption processes in which the free electrons and holes are photogenerated, and η is the number of carriers generated by one photon.

To simplify (2) the authors of this paper have assumed additional conditions: surface recombination velocities on the front and back surfaces of the sample are equal (i.e. $S_1 = S_2 = S$), the absorption coefficient α is large in comparison to the diffusion length L ($\alpha L \gg 1$) and the sample thickness w is much greater than L ($w/L \gg 1$). These assumptions are consistent with the described experiments. The resulting equation which describes the spectral dependence of photoconductivity is the following:

$$\sigma_{PC}(h\nu) = eI_0[1 - R_0(h\nu)]\beta(h\nu)A_{PC}\left(\frac{1}{S} + \frac{1}{\alpha\,(h\nu)\,w}\right) \tag{4}$$

where $A_{PC} = (\mu_n + \mu_p)\frac{\tau}{L}$, τ is the bulk lifetime, and R_0 the reflectivity coefficient.

Normalized spectral dependences of photoconductivity (e.g. the presented in figure 12) have been least-squares fitted using equation (4) for each temperature and for different light intensities. The fitting was performed for photon energies characteristic for intrinsic photogeneration. In this spectral range the values of the quantum efficiency coefficient can be assumed as equal: $\beta = 1$ (see e.g. [8]). For the least-squares fitting the numerical method presented in [14] was used. Using the values of the fitted parameters A_{PC} and S (table 1 and 2) the theoretical $\sigma_{PCcalc}(h\nu)$ characteristics were calculated in the full spectral range in which σ_{PC} was measured and the values of absorption coefficients had been obtained (figure 12). Because

Table 1. Values of the parameter A_{PC} from equation (4) obtained from the fitting of σ_{PC} data normalized for different illumination intensities and GaS temperatures.

	I_0 (10^{17} photons m^{-2} s^{-1})			
T (K)	2	4	6	8
	A_{PC} (10^{-8} m V^{-1})			
333	4.73 ± 0.42	2.86 ± 0.25	2.13 ± 0.19	1.72 ± 0.15
293	1.53 ± 0.16	1.16 ± 0.12	0.98 ± 0.11	0.86 ± 0.09
238	3.8 ± 0.4	2.99 ± 0.31	2.45 ± 0.25	2.14 ± 0.22
203	2.05 ± 0.14	2.30 ± 0.15	1.91 ± 0.13	1.58 ± 0.11
173	2.23 ± 0.23	1.9 ± 0.2	1.63 ± 0.17	1.45 ± 0.15
150	3.52 ± 0.25	3.29 ± 0.23	3.19 ± 0.23	3.13 ± 0.22
135	2.02 ± 0.19	1.78 ± 0.17	1.65 ± 0.16	1.56 ± 0.15
120	4.07 ± 0.35	3.55 ± 0.31	3.24 ± 0.28	3.03 ± 0.26
80	4.88 ± 0.56	5.14 ± 0.59	5.25 ± 0.61	5.31 ± 0.61

Table 2. Values of the dimensionless surface recombination velocities S from equation (4) obtained from the fitting of σ_{PC} data normalized for different illumination intensities and GaS temperatures.

	I_0 (10^{17} photons m^{-2} s^{-1})			
T (K)	2	4	6	8
	S			
333	1.142 ± 0.038	1.239 ± 0.041	1.388 ± 0.046	1.644 ± 0.055
293	0.160 ± 0.011	0.181 ± 0.013	0.210 ± 0.015	0.259 ± 0.019
238	0.829 ± 0.052	0.978 ± 0.062	1.290 ± 0.081	2.38 ± 0.15
203	0.163 ± 0.018	0.257 ± 0.029	0.473 ± 0.053	1.49 ± 0.17
173	0.157 ± 0.023	0.201 ± 0.029	0.277 ± 0.041	0.444 ± 0.064
150	0.52 ± 0.12	0.52 ± 0.12	0.52 ± 0.12	0.54 ± 0.13
135	0.215 ± 0.021	0.146 ± 0.013	0.163 ± 0.015	0.191 ± 0.017
120	0.226 ± 0.017	0.249 ± 0.018	0.284 ± 0.021	0.341 ± 0.025
80	0.249 ± 0.014	0.232 ± 0.013	0.212 ± 0.012	0.187 ± 0.011

the assumed $\beta = 1$ is unrealistic for photon energies smaller than the energy gap, $\sigma_{PCcalc}(h\nu)$ in the corresponding spectral range considerably exceeds the experimental data (figure 12).

Then the quantum efficiency coefficient was calculated as the normalized ratio of the measured σ_{PC} to the theoretically evaluated σ_{PCcalc} photoconductivity:

$$\beta(h\nu) = \frac{\sigma_{PC}(h\nu, T, I_0)}{\sigma_{PCcalc}(h\nu, T, I_0)\beta_{MAX}} \tag{5}$$

where β_{MAX} represents the maximum value of $\beta(h\nu)$. In this study it was assumed that $\beta_{MAX} = (\frac{\sigma_{PC}(h\nu,T,I_0)}{\sigma_{PCcalc}(h\nu,T,I_0)})_{MAX} = 1$ for photon energy higher than that for which σ_{PC} attains maximum and smaller than the double energy gap. The results of the performed evaluations of $\beta(h\nu)$ are presented in figures 13 and 14. The first figure shows the spectral characteristics of the coefficient β for different illumination intensities. The second one presents the influence of temperature on spectral dependences of β values averaged for different illumination intensities. The decrease of temperature causes a shift of the spectral dependences of β along the $h\nu$ axis to higher energies. It is consistent with changes of the energy gap of GaS.

Knowing the value of $\beta(h\nu)$, one can calculate the values of $\alpha_\beta(h\nu)$ using (3) and assuming $\eta = 1$ (figure 15). This method of evaluating $\alpha_\beta(h\nu)$ is similar to the one used

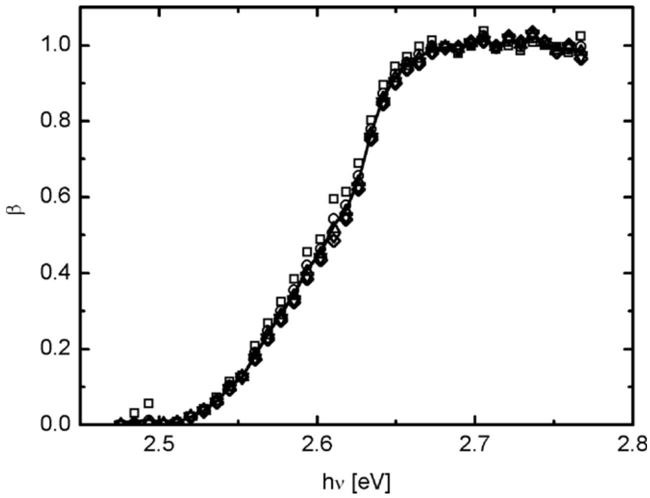

Figure 13. The quantum efficiency coefficient β for photogeneration of excess carriers as a function of photon energies at temperature $T = 80$ K in GaS for different illumination intensities ((□) $I_0 = 2 \times 10^{17}$ photons m^{-2} s^{-1}, (O) $I_0 = 4 \times 10^{17}$ photons m^{-2} s^{-1}, (Δ) $I_0 = 6 \times 10^{17}$ photons m^{-2} s^{-1}, (▽) 8×10^{17} photons m^{-2} s^{-1}, (◇) 10^{18} photons m^{-2} s^{-1}). The solid curve represents the value of β averaged for different illumination intensities.

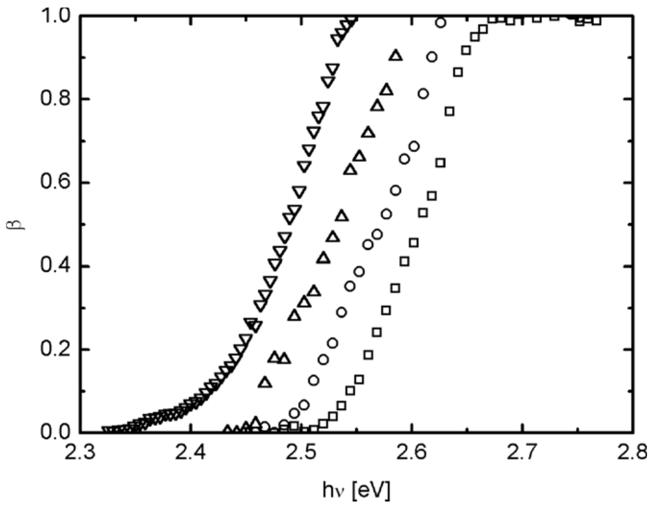

Figure 14. The quantum efficiency coefficient β for photogeneration of excess carriers in GaS as a function of photon energies for different temperatures ((□) $T = 80$ K, (O) $T = 150$ K, (Δ) $T = 203$ K, (▽) $T = 333$ K).

in [6, 7]. It should be noted that the photocurrent can be used to monitor the radiation absorption coefficient by applying for example the method suggested by Moddel *et al* [15] or the constant photocurrent method (CPM) [16]. Comparison of the methods was given in [6].

In figure 15 the estimated spectral dependences of $\alpha_\beta(h\nu)$ are compared with $\alpha(h\nu)$ for temperatures $T = 333$, 238 and 80 K. It can be seen that for photon energies below 2.63 eV at $T = 80$ K, below 2.55 eV at 238 K and below 2.5 eV at $T = 333$ K the total absorption of light in GaS is greater than the absorption that evokes photogeneration of free electrons and holes.

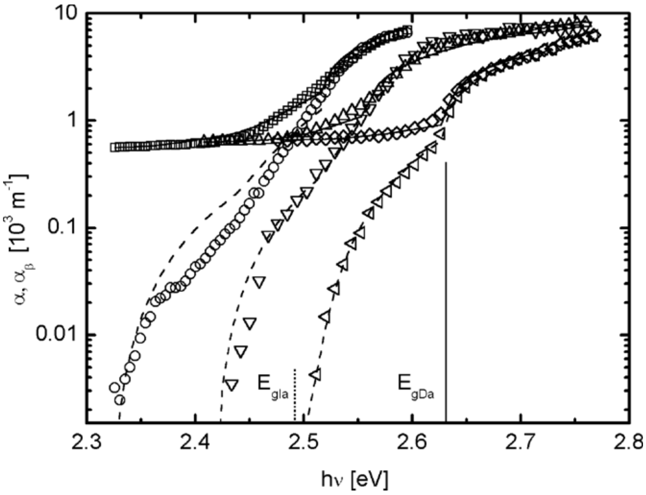

Figure 15. Spectral dependence of total absorption coefficient $\alpha(h\nu)$ (□, Δ, ◇) and absorption coefficient $\alpha_\beta(h\nu)$ (○, ▽, ◁) describing absorption processes in which the free electrons and holes are photogenerated in GaS at $T = 333$ K (□, ○), $T = 238$ K (◇, ◁) and $T = 80$ K (Δ, ▽), respectively. Solid and dot curves represent theoretical dependences (6) calculated for the fitted values of E_{gIa}, E_{gDa}, E_{ph} (see figures 16 and 17). Vertical lines described as E_{gIa} and E_{gDa} show the determined indirect and direct energy gap of GaS at 80 K.

The spectral dependences $\alpha_\beta(h\nu)$ estimated for different temperatures, as well as $\alpha(h\nu)$, were least-squares fitted with theoretical equations describing different absorption processes. The best results were obtained assuming

$$\alpha(h\nu) = \alpha_0(h\nu) + \alpha_{\mathrm{D}}(h\nu) + \alpha_{\mathrm{I}}(h\nu) \quad (6)$$

where $\alpha_D(h\nu)$ represents direct allowed absorption without excitons, normalized for $h\nu$ [17, 18], and $\alpha_I(h\nu)$ represents indirect allowed absorption with absorption/emission of phonons without excitons, normalized for $h\nu$ [13, 17, 19]; α_0 is the additive constant [20]. Therefore

$$\alpha_{\mathrm{D}} = 0 \qquad \text{for } h\nu \leqslant E_{\mathrm{gDa}} \quad (6a)$$

$$\alpha_{\mathrm{D}} = \frac{C_1}{h\nu}\sqrt{h\nu - E_{\mathrm{gDa}}} \qquad \text{for } h\nu > E_{\mathrm{gDa}} \quad (6b)$$

$$\alpha_{\mathrm{I}} = 0 \qquad \text{for } h\nu \leqslant E_{\mathrm{gIa}} - E_{\mathrm{ph}} \quad (6c)$$

$$\alpha_{\mathrm{I}} = \frac{C_2}{h\nu}\frac{(h\nu - E_{\mathrm{gIa}} + E_{\mathrm{ph}})^2}{\exp\left(\frac{E_{\mathrm{ph}}}{k_{\mathrm{B}}T}\right) - 1} \qquad \text{for } E_{\mathrm{gIa}} - E_{\mathrm{ph}} < h\nu \leqslant E_{\mathrm{gIa}} + E_{\mathrm{ph}} \quad (6d)$$

$$\alpha_{\mathrm{I}} = \frac{C_3}{h\nu}\left\{\frac{(h\nu - E_{\mathrm{gIa}} + E_{\mathrm{ph}})^2}{\exp\left(\frac{E_{\mathrm{ph}}}{k_{\mathrm{B}}T}\right) - 1} + \frac{(h\nu - E_{\mathrm{gIa}} - E_{\mathrm{ph}})^2}{1 - \exp\left(-\frac{E_{\mathrm{ph}}}{k_{\mathrm{B}}T}\right)}\right\} \qquad \text{for } h\nu > E_{\mathrm{gIa}} + E_{\mathrm{ph}} \quad (6e)$$

where E_{gDa}, E_{gIa} represent the direct allowed and indirect allowed energy gaps, E_{ph} is the effective phonon energy, k_B the Boltzmann constant, and C_1, C_2, C_3 proportionality constants.

In the fitting of $\alpha_\beta(h\nu)$, the values of α_0 turned out to be zero. Figures 16 and 17 present the fitted values of energy gaps and phonons energies for different temperatures. Solid and dotted curves in figure 15 show the theoretical absorption (6) calculated using the fitted values of E_{gDa}, E_{gIa} and E_{ph}. The fitting is rather good. One should notice that the values of direct and

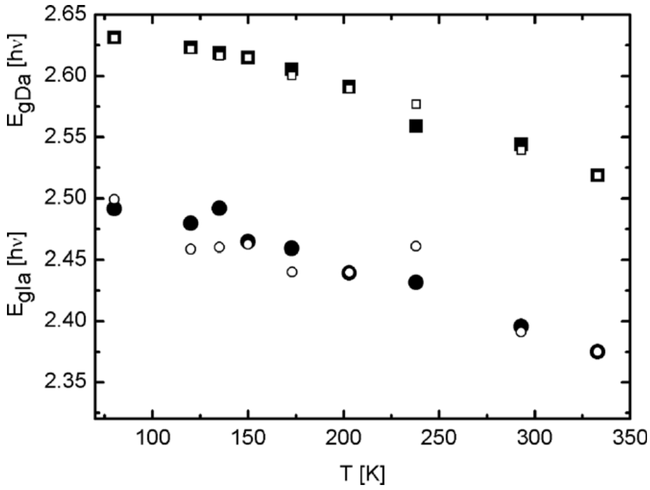

Figure 16. Temperature dependence of the energy gap of GaS determined from spectral characteristics of the absorption coefficient, evaluated from transmittance and reflectance data (■, ●) and from photoconductivity data, i.e. from quantum efficiency coefficients for photogeneration of carriers (□, ○). The symbols (■), (□) represent the direct energy gap, E_{gDa}, and (●), (○) the indirect energy gap, E_{gIa}.

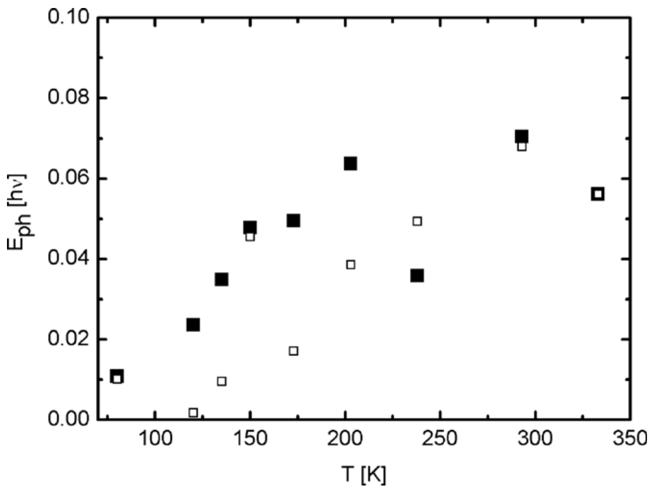

Figure 17. Temperature dependence of effective phonon energies determined from spectral characteristics of the absorption coefficient, evaluated from transmittance and reflectance data (■) and from photoconductivity data (quantum efficiency coefficients for photogeneration of carriers) (□).

indirect energy gaps evaluated from quite different experimental results (optical transmittance and reflectance as well as photoconductivity) are practically the same (figure 16).

5. Conclusions

The temperature and spectral dependences of the $\gamma(h\nu, T)$ coefficient of the power-law dependence of photoconductivity on illumination intensity as well as the temperature and spectral dependences of quantum coefficient for photogeneration of carriers, determined for the first time for gallium sulphide (GaS), may be useful in the optimization of photoelements produced from this semiconductor.

The nonlinear recombination of carriers in GaS at temperatures higher than 200 K needs future investigations that should result in the determination of energetic positions, concentrations and cross-sections of electron states in the energy gap of this material.

The values of energy gaps (direct allowed and indirect allowed) of GaS at different temperatures determined from the spectral dependences of absorption coefficient evaluated from optical transmittance and reflectance as well as from quantum coefficient for photogeneration of carriers compare well with each other. However, it should be stressed that $\alpha_\beta(h\nu)$ was fitted with $\alpha_I(h\nu) + \alpha_D(h\nu)$ while $\alpha(h\nu)$ needs the sum of $\alpha_\mathrm{I}(h\nu) + \alpha_\mathrm{D}(h\nu) + \alpha_0(h\nu)$ for fitting. Of course a smaller number of parameters involved in the description of the absorption coefficient $\alpha_\beta(h\nu)$ allows one to determine the absorption mechanisms and their parameters more reliably. The values of E_gIa and E_gDa determined can be compared with the literature data. Unfortunately these data are only available for a few temperatures. The values of E_gIa determined in this paper are about 2%–6% lower than the values obtained in, for example, [11, 21, 22] for temperatures 77, 150 K and for room temperature. The values of E_gDa are about 8% smaller than the data in [21] for $T = 77$ K and for room temperature. Unfortunately, the value of E_gDa obtained in [11] for room temperature is about 15% greater than that evaluated in this paper. However, it should be noticed that the literature data were obtained for total absorption. One can expect that the data presented here are more reliable.

The comparison of the absorption coefficients $\alpha(h\nu, T)$ and $\alpha_\beta(h\nu, T)$ allows one to distinguish the absorption process which produces the free carriers as well as the other absorption or scattering mechanisms.

The approach to the investigation of optical and photoelectrical properties of GaS presented in this paper can also be useful in examinations of other semiconductors.

Acknowledgments

The authors thank Professor R Murri from the University of Camerino (Italy) and Professor V Augelli from the University of Bari (Italy) for providing us with samples of gallium sulphide. This work was partially financed by the Silesian University of Technology, Gliwice (Poland) under contract BW/RMF-1/2006.

References

[1] Aydinli A, Gasanly N M and Goksen K 2000 *J. Appl. Phys.* **88** 7144–9
[2] Brodin S and Blonskii I W 1986 *Exciton Processes in Layer Crystals* (Kijev: Naukova Dumka) (in Russian)
[3] Kuroda N, Nishina Y and Fukuroi T 1970 *J. Phys. Soc. Japan* **28** 981–92
[4] Brebner J L 1964 *J. Phys. Chem. Solids* **25** 1427–33
[5] Moss T S 1954 The photo electro-magnetic effect in geranium and lead sulphide *Physica* **20** 989–93
[6] Grabowski A, Nowak M and Tzanetakis P 1996 *Thin Solid Films* **283** 75
[7] Augelli V, Murri R and Nowak M 1989 *Phys. Rev.* B **39** 8336
[8] Drapak S I, Bakhtinov A P, Drapak I T, Kovalyuk Z D and Tovarnitsky M V 2005 *J. Optoelectron. Adv. Mater.* **7** 801–4
[9] Kipperman A H M and Leeden G A 1968 *Solid State Commun.* **6** 657–62
[10] Manfredotti C, Murri R, Rizzo A and Vasanelli L 1976 *Solid State Commun.* **19** 339–42
[11] Manfredotti C, Rizzo A, Bufo A and Cardetta V L 1975 *Phys. Status Solidi* a **30** 375–82
[12] Gärtner W 1957 *Phys. Rev.* **105** 823–9
[13] Pankove J I 1971 *Optical Processes in Semiconductors* (Englewood Cliffs, NJ: Prentice-Hall)
[14] Kończak S and Nowak M 1981 *Phys. Status Solidi* a **68** 305
[15] Moddel G, Anderson D A and Paul W 1980 *Phys. Rev.* B **22** 1918
[16] Vanecek M, Kocka J and Stulik J 1981 *Solid State Commun.* **39** 1199
[17] El-Korashy A and Abu El-Fadl A 1999 *Physica* B **271** 205–11
[18] Gürbulak B 2001 *Physica* B **293** 289–96
[19] Hasegawa T, Shirai M and Tanaka K 2000 *J. Lumin.* **87–89** 1217–9
[20] Johnson S R and Tiedje T 1997 *J. Cryst. Growth* **175/176** 273–80
[21] Kępińska M, Nowak M, Szałajko M and Murri R 2001 *J. Wide Bandgap Mater.* **8** 241–9
[22] Brebner J L and Fischer G 1963 *Can. J. Phys.* **41** 561–3